

Monomer Basis Representation Method For Calculating The Spectra Of Molecular Clusters II. Application To Water Dimer.

Mahir E. Ocak*

Yaşamkent Mahallesi, Yonca Sitesi 13/B Daire No:5, Çayyolu, Ankara, Turkey

(Dated: June 15, 2021)

Abstract

The Monomer Basis Representation (MBR) method developed in the first paper is applied to water dimer in order to illustrate its application and to show its validity. The calculations are done by using the SAPT-5st potential surface. Monomers are treated as rigid bodies. Radial coordinate is separated from the angular coordinates adiabatically. MBR method is used for solving the five dimensional angular problem. Then, the results of the angular calculations are fit to a Morse function to find the potential surface for the radial motion. The results show that the method works efficiently and accurately.

*Electronic address: meocak@alumni.uchicago.edu

I. INTRODUCTION

Water clusters have been the subject of intense research in the literature, since they are important for understanding hydrogen bonding, for interpreting the many special features of the structure, dynamics and energetics of bulk solid and liquid water. Besides hydrogen bonding to water molecules is of general importance in many biological, chemical and physical systems.

Theoretical studies of small water clusters shows that many-body terms are very important. For water, it is known that many-body terms may account for up to 25% of the interaction energy of the bulk water [1]. It has been found that [2]: the pair interaction energy represents 83 – 86% of the total interaction energy of $(H_2O)_3$. For $(H_2O)_4$ the same percentage amounts to $\approx 75\%$, for $(H_2O)_5$ only to $\approx 68\%$. It is evident that many-body terms are far from negligible. It has also been found that the major part of the many-body cooperative effect comes from three-body terms. The four-body terms represent 2% of the total interaction energy of the $(H_2O)_4$, and less than 4% of the total interaction energy of the $(H_2O)_5$. Therefore, characterization of three body terms is a major step for the development of an accurate potential surface for bulk liquid and solid water.

Before starting to work on three-body terms, first it is necessary to have an accurate description of the two body terms in the potential surface. For that purpose, water dimer has been studied extensively both experimentally [3–16] and theoretically [17–24], and many potential surfaces has been developed [25–33].

Among the theoretical studies of water dimer, Clary and co-workers were the first ones to perform six dimensional calculations. Firstly, Althorpe and Clary studied water dimer by separating the stretching coordinate from the angular coordinates adiabatically [17]. This adiabatic approximation was justified later with a more exact treatment [22]. In the calculations, Wigner rotation functions were used as angular basis for each monomer, and the molecular symmetry of water dimer was fully exploited. Later, the same authors developed a new method named Discrete Variable Representation Iterative Secular Equation (DVR-ISE) which is an extension of the diagonalization truncation method by using the variation-perturbation theory. The method utilizes the iterative secular equation (ISE) method [34]. In the calculations, functional bases were used for some of the angles and DVR bases were used for the other angles. Later, Gregory and Clary studied water dimer [19] with Diffusion

Monte Carlo (DMC) method [35, 36]. Leforestier and co-workers were the first ones to do fully coupled six dimensional calculations with basis sets. They published two papers [20, 21]. The first one included some erroneous data because of a mistake in the moments of inertia of water monomers which were being corrected in the second one. The calculations were done with a coupled product basis of Wigner rotation functions by using the pseudospectral split Hamiltonian (PSSH) formalism in which the kinetic energy terms are evaluated in the coupled product basis of Wigner rotation functions and the potential energy is evaluated in the grid basis. Later, Chen and Light also made fully coupled six dimensional calculations of water dimer [22] by using the sequential diagonalization truncation method in which angular and the radial parts of the Hamiltonian were diagonalized successively. In these calculations, authors used the same decoupled product basis of Wigner rotation functions with the first calculations of Althorpe and Clary [17], and the symmetry of water dimer was exploited fully in calculations. Results showed that the adiabatic approximation of the Althorpe and Clary is successful for predicting the tunneling splittings. Finally, van der Avoird and co-workers developed a new potential surface called SAPT-5s [23] by using the Symmetry Adapted Perturbation Theory (SAPT) [2, 37, 38]. This potential surface was tuned for predicting the vibration-rotation-tunneling levels of water dimer which led to the development of a new potential surface called SAPT-5st [24]. The tuned potential surface describes the experimental data with near spectroscopic accuracy [23, 24, 39]. In calculations, first an equally spaced grid was taken for the stretching coordinate and the angular Hamiltonian was solved at 49 different grid points by using a coupled product basis of Wigner rotation functions. Then, a three point contracted DVR [40] basis were used for the stretching coordinate.

Since some experimental data about water trimer is available [41–47], many researchers started to work on water trimer [48–57]. However, since the size of the water trimer problem is too big to handle quantum mechanically, all the theoretical studies done up to now are based on very reduced dimensionality models, even for rigid water molecules. The method developed in the first paper may make it possible to study clusters as big as water trimer with more realistic models as it will be seen.

In the following section, the MBR method developed in the first paper will be used for calculating the vibration-rotation-tunneling (VRT) spectra of water dimer in order to illustrate the application of the method, and to show its validity. In calculations, adiabatic

approximation of Althorpe and Clary, PSSH formalism of Leforestier and co-workers and the potential surface of Groenenboom *et. al.* will be used. The main difference of the calculations here from the previous calculations is the generation of optimized bases for each monomer in the cluster by using the MBR method. It will be seen that the use of the MBR method leads to successful results with a basis which has a much smaller size than any of the bases used in previous studies of water dimer.

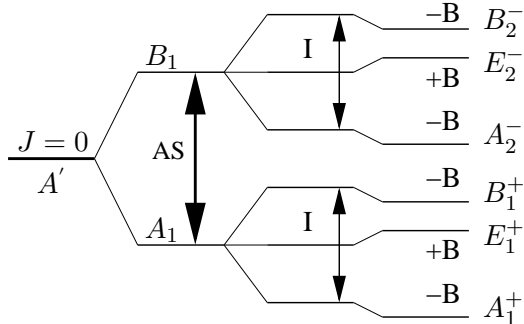
II. STRUCTURE OF WATER DIMER

Water clusters are highly nonrigid, even with rigid monomers. Their potential surface contains more than one global minimum which are equivalent by symmetry. The potential barriers between these minima are not high, so that the molecule can tunnel through these barriers which causes tunneling splittings in the vibration-rotation-tunneling (VRT) spectra of the molecules. Calculation of these splittings is a good test for the accuracy of the available potential surfaces. Since the wave functions corresponding to the splitting levels has considerable amplitude in the region where the tunneling occurs, a good prediction of the tunneling splittings shows that the potential surface used in the calculations is accurate not only around the minimum (which is usually the case when there is no tunneling) but also in the tunneling region.

The structure of water dimer was first determined by Dyke and co-workers via rotation spectra [3, 4]. By examining the experimental data, Dyke realized the presence of tunneling splittings and made a group theoretical classification of the tunneling-rotational levels [58] by using Permutation Inversion (PI) group theory [59, 60]. It was shown that, the equilibrium structure of water dimer has a plane of symmetry and a nonlinear hydrogen bond. The equilibrium structure of water dimer is depicted roughly in figure 2. The $O - O$ distance reflecting the length of the H-bond is 2.952 Å, and the dissociation energy of the hydrogen bond, D_e is 3.09 kcal/mole [43].

By including all feasible permutation inversion operations it is possible to generate 16 different configurations. Due to the presence of a plane of symmetry in the equilibrium structure, there is twofold structural degeneracy and only eight of these structures are non-superimposeable. There exist three distinct tunneling motions that rearrange the H-bond network on time scales ranging from 1 μ s to 1 ps [61]. The tunneling motions connect eight

FIG. 1: Correlation diagram for the rotation-tunneling states of $(H_2O)_2$ for $J = 0$. In the figure AS, I and B refers to acceptor switching, interchange tunneling and bifurcation tunneling respectively. Levels are labeled with the irreducible representations of the G_{16} PI group.



degenerate minima on the intermolecular potential surface (IPS). These tunneling motions are acceptor switching (AS), interchange tunneling (I) and bifurcation tunneling (B).

Acceptor switching has the smallest barrier for the tunneling. In that motion the protons of the acceptor monomer exchange their positions. This tunneling does not break the hydrogen bond. Its causes splitting of each ro-vibrational level into two levels.

Interchange tunneling interchanges the roles of the acceptor and donor monomers. This motion has the second lowest barrier and it causes further splitting of the ro-vibrational levels.

Bifurcation tunneling has the highest barrier. Since acceptor switching and interchange tunneling, together with the inversion of the dimer, resolves all the degeneracy of the water dimer. The effect of the bifurcation tunneling is not to split the energy levels, but just to shift them. This is a result of the fact that water dimer has a plane of symmetry, which causes two fold structural degeneracy of each ro-vibrational level. Acceptor switching, interchange tunneling and the inversion of the dimer already connects eight degenerate minima to each other.

The splittings for $J = 0$ rotational level of water dimer are shown in figure 1. Each energy level is labeled with the irreducible representations of the G_{16} PI group which is the molecular symmetry group of water dimer.

III. HAMILTONIAN AND THE OUTLINE OF CALCULATION STRATEGY

The full water dimer problem is too big to handle quantum mechanically. Therefore, it is necessary to model the problem. In weakly bound clusters, inter-molecular and intra-molecular degrees of freedom have frequencies which differ by at least one order of magnitude. As a result of that inter-molecular and intra-molecular degrees of freedom can be separated adiabatically. Thus, while treating the inter-molecular degrees of freedom, the monomers can be considered as rigid bodies.

The Hamiltonian for the inter-molecular motion of a nonrigid system consisting of two rigid polyatomic fragments can be written as [62]

$$\hat{H} = -\frac{1}{2\mu R} \frac{\partial^2}{\partial R^2} R + \hat{K}_1 + \hat{K}_2 + \hat{K}_{12} + \hat{V}. \quad (1)$$

In the equation above, R is the distance between the centers of mass of the monomers. μ is the reduced mass of the dimer given by

$$\frac{1}{\mu} = \frac{1}{M_1} + \frac{1}{M_2}, \quad (2)$$

where M_i is the total mass of the monomers.

In the Hamiltonian \hat{K}_i is the kinetic energy operator of the monomer, which can be expressed in the body fixed frame of the monomer as

$$\hat{K}_i = A\hat{j}_{ix}^2 + B\hat{j}_{iy}^2 + C\hat{j}_{iz}^2, \quad (3)$$

in terms of the angular momentum operators around the body fixed axis of the monomer, which is the molecular symmetry axis in this case. For calculations, the z axis is defined to be the bisector of the HOH angle. The plane of the molecule is defined to be the xz plane. Rotational constants A, B, C are given in terms of the moments of inertia as

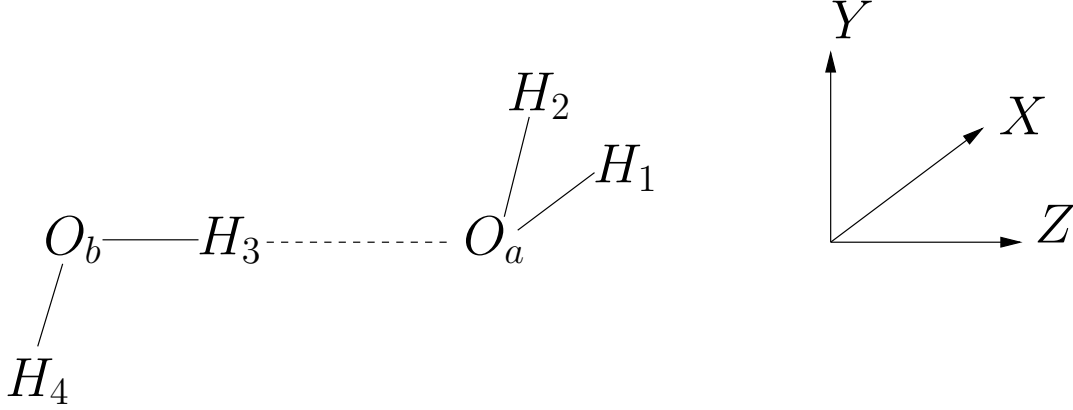
$$A = \frac{1}{2I_x}, \quad B = \frac{1}{2I_y}, \quad C = \frac{1}{2I_z}, \quad (4)$$

where I_x, I_y, I_z are the moments of inertia of the monomers around x, y, z axes respectively. Since the monomers are considered to be rigid A, B and C are constants.

In equation (1), \hat{K}_{12} defines the kinetic energy operator corresponding to the end-over-end rotation of the dimer. It is given by

$$\hat{K}_{12} = \frac{1}{2\mu R^2} (\hat{J}^2 + \hat{j}^2 - 2\hat{J} \cdot \hat{j}). \quad (5)$$

FIG. 2: Body fixed frame of water dimer.



In the equation above \hat{J} is the total angular momentum of the system given by

$$\hat{J} = \hat{j}_1 + \hat{j}_2 + \hat{L}, \quad (6)$$

where \hat{j}_i 's are the monomer angular momentum operators, and \hat{L} is the angular momentum operator for the end-over-end rotation of the dimer. \hat{j} is defined as $\hat{j} = \hat{j}_1 + \hat{j}_2$.

In order to evaluate the K_{12} term, it is necessary to express all the angular momentum operators in a common reference system. This reference system is the body fixed coordinate system of the dimer, of course. The z axis of the body fixed frame of the dimer is defined along the line joining the center of mass of the monomers and the y axis of the body fixed frame of the dimer is defined to be along the bisector of the HOH angle of the acceptor monomer in the equilibrium configuration; see figure 2. In this reference frame, K_{12} is expressed as

$$K_{12} = \frac{1}{2\mu R^2} (\hat{j}_1^2 + \hat{j}_2^2 + 2\hat{j}'_{1z}\hat{j}'_{2z} + \hat{j}'_{1+}\hat{j}'_{2-} + \hat{j}'_{2+}\hat{j}'_{1-} - 2\hat{J}'_z\hat{j}'_z - \hat{J}'_+\hat{j}'_- - \hat{J}'_-\hat{j}'_+). \quad (7)$$

For $J = 0$, this equation reduces to

$$K_{12} = \frac{1}{2\mu R^2} (\hat{j}_1^2 + \hat{j}_2^2 + 2\hat{j}'_{1z}\hat{j}'_{2z} + \hat{j}'_{1+}\hat{j}'_{2-} + \hat{j}'_{1-}\hat{j}'_{2+}). \quad (8)$$

In the equations above ' denotes that the operator refers to the body fixed frame of the dimer but not the body fixed frame of the monomers.

In order to solve the eigenvalue problem, first the stretching coordinate will be separated from the angular coordinates adiabatically. This is first done by Althorpe and Clary [17], and led to successful results.

First, the angular Hamiltonian is written in the form

$$\hat{H}_{ang} = \hat{h}_1^0 + \hat{h}_2^0 + \Delta\hat{K} + \Delta\hat{V} \quad (9)$$

where the model Hamiltonians, \hat{h}_i^0 , for the three dimensional monomer problems are given by

$$\hat{h}_i^0 = \hat{K}_i + \hat{V}_i^0 \quad (10)$$

in which \hat{K}_i is the monomer's kinetic energy operator in equation (1), and \hat{V}_i^0 is the model potential energy surface for the three dimensional problem, which is the rotation of the monomers.

By comparing equation (9) with the Hamiltonian, equation 1, it is easily seen that $\Delta\hat{K} = \hat{K}_{12}$ and $\Delta\hat{V}$ terms can be identified as

$$\Delta\hat{V} = \hat{V} - \hat{V}_1^0 - \hat{V}_2^0. \quad (11)$$

The results of the angular calculations will be used to find an effective potential surface for the radial coordinate so that the total Hamiltonian can be written as

$$\hat{H} = -\frac{1}{2\mu R} \frac{\partial^2}{\partial R^2} + V_{eff}(R). \quad (12)$$

Details of monomer calculations, five dimensional angular calculations and radial calculations will be given in sections IV, VII and VIII, respectively.

IV. GENERATION OF A MONOMER BASIS

A. Model Potential Surface

For solving the monomer problem, it is first necessary to chose a model potential surface. The choice here will be the external field which is generated by the other monomer.

When one wants to solve eigenstates of one monomer in the field of the other one, a natural question arises. Since the monomers in water dimer are not in the same environment their calculations will result in different eigenstates. Since the dimer includes both a donor and an acceptor, the results of neither calculation will generate a sufficient basis for solving the five dimensional angular problem. In order to handle this donor acceptor asymmetry of water dimer, the Energy Selected Basis (ESB) method will be used [63, 64].

In the ESB method, one generates the model potential surface as a marginal potential in which the potential energy at a point is the minimum value of the potential energy with respect to all other coordinates, i.e.

$$\hat{V}^0(q_k) = \hat{V}^0(q_k, q_{k'}^{min}). \quad (13)$$

Since the coordinates of the monomer which causes the external field is varied to find the minimum potential, the marginal potential will sample both the donor and the acceptor configurations. Therefore, the monomer calculation should result in a sufficient basis for both the donor and the acceptor monomers.

For solving water dimer problem with energy selected basis method, it is necessary to generate a three dimensional marginal potential. Labeling the monomers as i and j , the model potential for monomer i in the field of monomer j will be

$$\hat{V}_i^0(\zeta_i) = \hat{V}(\zeta_i, \zeta_j^{min}; R) \quad (14)$$

where $\zeta_i = (\alpha_i, \beta_i, \gamma_i)$ and $\zeta_j = (\alpha_j, \beta_j, \gamma_j)$ refer to the Euler angles of monomers which describe the orientation of the body fixed frame of the monomers with respect to the body fixed frame of the dimer.

B. Primitive Bases

In order to solve the problem two primitive bases will be used, one functional basis and one grid basis. Functional basis being small and compact will be the primary basis. Grid basis will be used for the evaluation of potential energy. Primitive functional basis will be the symmetric top basis $|jkm\rangle$. In this basis, j is the total angular momentum, k is the projection of angular momentum onto the body fixed z axis of the monomer and m is the projection of angular momentum on to the body fixed z axis of the dimer. Symmetric top basis functions can be expressed in terms of Wigner rotation functions as

$$|jkm\rangle = \frac{1}{2\pi} \sqrt{\frac{2j+1}{2}} D_{mk}^{j*}(\alpha, \beta, \gamma), \quad (15)$$

where $D_{mk}^j(\alpha, \beta, \gamma)$ is the the Wigner rotation function, expressed in terms of Euler angles α , β and γ . Its functional form is given by

$$D_{mk}^j(\alpha, \beta, \gamma) = e^{-im\alpha} d_{mk}^j(\cos \beta) e^{-ik\gamma}. \quad (16)$$

Exact functional form and the symmetry properties of the $d_{mk}^j(\cos \beta)$ function can be found elsewhere [65].

Following Light [66–68], the representation of the Hamiltonian in the symmetric top basis can be called Finite Basis Representation (FBR), and the representation of Hamiltonian in the grid basis can be called Discrete Variable Representation (DVR). The application of DVR methodology to non-product bases is discussed by Corey *et. al.* [69, 70] for the case of spherical harmonics, and later it is applied to the case of symmetric top basis [20, 21, 71]. The deviation from Light’s original formulation in the case of coupled bases is that one no longer seeks a unitary transformation between two bases. Therefore, two representations are no longer equivalent. Since the FBR basis is more compact it is the primary basis used in the calculations. Use of the DVR basis provides a simple way for the evaluation of potential energy matrix elements, since the potential energy matrix is diagonal in the DVR basis, and the matrix elements are given by the value of the potential energy at the corresponding grid point.

C. Symmetry Adaptation of Basis Functions

As discussed in the first paper, the monomer problem should be symmetry adapted to the direct product group of the pure permutation group of the monomer, and the inversion subgroup of the dimer. If one labels the hydrogen atoms as 1 and 2, then the pure permutation group of water monomers is the group $G_2 = \{E, (12)\}$. The inversion subgroup is as usual $\varepsilon = \{E, E^*\}$. In this case, the direct product group becomes isomorphic to the molecular symmetry group of free water monomers, which is $C_{2v}(M)$. However, the E^* operation here refers to the inversion of the full dimer system, and not to the inversion of free water monomers. Character table of the group $C_{2v}(M)$ is given in table I.

In order to make the symmetry adaptation of the basis functions, it is necessary to find the effects of the permutation inversion operations to Euler angles and to the basis functions. A simple way of finding the transformation properties of Euler angles is given in appendix A. By using the transformation properties given in that appendix and by defining the body fixed frame of the monomers as in figure 3 effect of the permutation operations to Euler angles can be found. The results are given in table IV. By using these transformations and the symmetry properties of the Wigner rotation functions, the effects of the permutation

TABLE I: Character table of the $C_{2v}(M)$ permutation inversion group. This group is the direct product of the groups G_2 , whose character table is given in table II, and ε , whose character table is given in table III. In the table, $\Gamma = x \otimes y$ means that the irreducible representation Γ of the group $C_{2v}(M)$ is obtained as direct product of the irreducible representation x of the group G_2 and the irreducible representation y of the group ε .

$C_{2v}(M) = G_2 \otimes \varepsilon$	E	(12)	E^*	$(12)^*$
$A_1 = A \otimes G$	1	1	1	1
$A_2 = A \otimes U$	1	1	-1	-1
$B_1 = B \otimes U$	1	-1	-1	1
$B_2 = B \otimes G$	1	-1	1	-1

TABLE II: Character table of the G_2 permutation group.

G_2	E	(12)
A	1	1
B	1	-1

TABLE III: Character table of the inversion group ε .

ε	E	E^*
G	1	1
U	1	-1

inversion operations to the symmetric top basis functions can also be found, the results are given in table IV.

By using the projection operators of the group $C_{2v}(M)$, whose character table is given in table I, symmetry adaptation of the basis functions can be done. The symmetry adapted basis functions will be in the form of

$$|jkm; p\rangle = N_p (|jkm\rangle + (-1)^p |j\bar{k}\bar{m}\rangle), \quad (17)$$

FIG. 3: Orientation of the body fixed frame of water monomers. Molecule is in the xz plane. Origin of the axes is the center of mass of the water molecule.

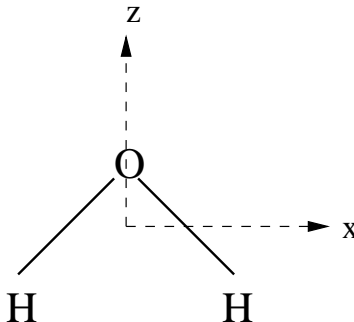


TABLE IV: Transformation properties of Euler angles under the effect of the symmetry operations of the $C_{2v}(M)$ molecular symmetry group and the effect of the permutation inversion operations to symmetric top basis functions.

E	α	β	γ	$ jkm\rangle$
(12)	α	β	$\pi + \gamma$	$(-1)^k jkm\rangle$
E^*	$\pi - \alpha$	β	$-\gamma$	$(-1)^k j\bar{k}\bar{m}\rangle$
(12)*	$\pi - \alpha$	β	$\pi - \gamma$	$ j\bar{k}\bar{m}\rangle$

with the normalization constant given by,

$$N_p = \frac{1}{2(1 + \delta_{k0}\delta_{m0})}. \quad (18)$$

In equation (17), p is either 0 or 1, and k is either even or odd depending on the symmetry. Table V gives the values of the parameter p for each symmetry level.

Symmetry adaptation of the grid basis can also be done. Construction of a grid basis for Wigner rotation functions is discussed by Leforestier [20, 21, 71]. According to his prescription, the grid basis that corresponds to an FBR basis of symmetric top basis is a uniform grid for the angles α and γ whose range is $(0, 2\pi)$, and Gauss-Legendre quadrature points for $\cos\beta$ whose range is $(-1, 1)$. This choice of grid basis corresponds to a direct product basis of plane wave DVR bases in angles α and γ and a Gauss-Legendre DVR basis in $\cos\beta$.

The construction of symmetry adapted DVR functions is discussed by Light and Car-

TABLE V: Partitioning of the symmetry adapted monomer basis for the monomer calculations. Form of the basis functions is given in equation (17).

Representation	p	k
A_1	0	even
A_2	1	even
B_1	0	odd
B_2	1	odd

rington [68]. There are two approaches. First approach is to find the symmetry adapted DVR functions by diagonalizing a symmetric function of the coordinate in an FBR basis which has the desired symmetry properties [72]. Second approach is to find the DVR basis functions by first using the usual procedure and then to obtain the symmetry adapted DVR functions as linear combinations of primitive DVR functions by using the well known projection operators technique. This method is first used by Carrington [73, 74]. If the application of symmetry operations mixes different coordinates, then the first approach is not applicable. It is also not applicable at all, if the primitive basis is not a direct product basis.

Since the symmetric top basis is a coupled basis, the first method mentioned above is not applicable. Therefore, the symmetry adapted DVR functions should be constructed by symmetry adapting the primitive DVR functions.

Before discussing the symmetry adaptation of the grid basis, let's define $|\alpha_i\rangle$, $|\beta_j\rangle$, $|\gamma_k\rangle$, as the basis functions which are localized around the points α_i , β_j and γ_k for the angles α , β , and γ respectively. Then,

$$|\alpha_i\beta_j\gamma_k\rangle = |\alpha_i\rangle|\beta_j\rangle|\gamma_k\rangle, \quad (19)$$

represents a direct product basis function in the grid basis. The transformation properties of the Euler angles given in table IV requires that if α_i and γ_k are grid points than $\pi - \alpha_i = \bar{\alpha}_i$, $\pi + \gamma_k = \gamma_k^*$, $-\gamma_k = \bar{\gamma}_k$ and $\pi - \gamma_k = \bar{\gamma}_k^*$, should also be grid points.

Since the group $C_{2v}(M)$ is the direct product of the group G_2 whose character table is given in table II and the inversion group ε whose character table is given in table III; symmetry adaptation of the basis functions can be done in two steps by first symmetry

adapting to the irreducible representations of the group G_2 and then symmetry adapting to the irreducible representations of the group ε .

Effect of the (12) operation to the Euler angles is given in table IV. With this transformation DVR basis functions symmetry adapted to the G_2 permutation group can be written as

$$|\alpha_i\beta_j\gamma_k; s\rangle = \frac{1}{\sqrt{2}} (|\alpha_i\beta_j\gamma_k\rangle + (-1)^s |\alpha_i\beta_j\gamma_k^*\rangle). \quad (20)$$

In this equation, the parameter s depends on the specific symmetry such that $(-1)^s$ becomes the character of the (12) operation in the irreducible representation that the basis function belongs to. The symmetry adaptation to the G_2 permutation group reduces the range of the angle γ by a half so that the range of angle γ becomes

$$0 \leq \gamma_k < \pi. \quad (21)$$

Basis Functions can also be symmetry adapted to the inversion subgroup of the molecular symmetry group of the water dimer. In this case, symmetry adapted basis functions will be in the form of

$$|\alpha_i\beta_j\gamma_k; sl\rangle = N_l (|\alpha_i\beta_j\gamma_k; s\rangle + (-1)^l |\bar{\alpha}_i\beta_j\bar{\gamma}_k; s\rangle), \quad (22)$$

where the normalization constant is given by,

$$N_l = \frac{1}{\sqrt{2(1 + \delta_{\alpha_i\bar{\alpha}_i}\delta_{\gamma_k\bar{\gamma}_k})}}. \quad (23)$$

The symmetry adaptation to the inversion subgroup of the molecular symmetry group of the dimer reduces the range of α by a half so that the range of α becomes

$$\frac{\pi}{2} \leq \alpha_i \leq \frac{3\pi}{2}. \quad (24)$$

The symmetry adapted DVR functions can be obtained for each irreducible representation of the group $C_{2v}(M)$ by taking different combinations of the parameters s and l . The values of the parameters s and l are given in table VI for each irreducible representation.

Before closing this section a few points about the partitioning of the grid basis should be mentioned. The grid points in β are obtained as the DVR points of Gauss-Legendre DVR of $\cos\beta$ by using the standard procedure [68, 75]. The DVR points in $\cos\beta$ are distributed symmetrically with respect to $\beta = \pi/2$.

TABLE VI: Values of the parameters s and l for the symmetry adapted grid basis.

Representation	s	l
A_1	0	0
A_2	0	1
B_1	1	1
B_2	1	0

In the case of the angles α and γ , grid points are evenly and periodically distributed between 0 and 2π . Thus, the grid points of the angles α and γ which are the plane wave DVR points are given by

$$\phi_j = j \left(\frac{2\pi}{N} \right) \quad (25)$$

where ϕ is either α or γ , N is the number of DVR points and $j = 0, 1, \dots, N-1$. According to this prescription 0 is always a grid point. As a result of that, the transformation properties of Euler angles given in table VII, requires that π should always be a grid point, too. According to equation (25), this is possible only if N is an even number. Therefore, N should be an even number in calculations.

D. Transformation Matrix And The Evaluation of Potential Energy Matrix Elements

The use of DVR provides a simple way for the evaluation of potential energy, since the potential matrix is diagonal in the DVR basis. However, in the case of coupled bases FBR basis is more compact, so that it is the primary basis used in the calculations. Consequently, one needs to transform the potential matrix from the DVR basis to the FBR basis, so that the total Hamiltonian can be evaluated as

$$H^{(FBR)} = K^{(FBR)} + V^{(FBR)} = K^{(FBR)} + T^\dagger V^{(DVR)} T. \quad (26)$$

The way to define the transformation matrix between the symmetric top basis and the corresponding grid basis is discussed by Leforestier [71]. The transformation matrix elements

between the symmetric top basis, $|jkm\rangle$, and the grid basis are given by

$$T_{\alpha_i\beta_j\gamma_k}^{jkm} = \sqrt{\frac{2j+1}{2}} \frac{e^{im\alpha_i}}{\sqrt{N_\alpha}} \frac{e^{ik\gamma_k}}{\sqrt{N_\gamma}} \sqrt{w_{\beta_j}} d_{mk}^j(\cos\beta_j), \quad (27)$$

where N_α and N_γ are the number of grid points for the angles α and γ , w_{β_j} is the weight of the grid point β_j of the Gauss-Legendre quadrature for $\cos\beta$. Thus, the DVR basis functions are defined as

$$\delta_{\alpha_i\beta_j\gamma_k}(\alpha, \beta, \gamma) = \sum_{jkm} |jkm\rangle T_{\alpha_i\beta_j\gamma_k}^{jkm} \quad (28)$$

$$= \sum_{jkm} \frac{1}{2\pi} \sqrt{\frac{2j+1}{2}} D_{mk}^{j*}(\alpha, \beta, \gamma) T_{\alpha_i\beta_j\gamma_k}^{jkm} \quad (29)$$

$$= \sum_{jkm} \frac{2j+1}{4\pi} \frac{e^{im\alpha_i}}{\sqrt{N_\alpha}} \frac{e^{ik\gamma_k}}{\sqrt{N_\gamma}} \sqrt{w_{\beta_j}} d_{mk}^j(\cos\beta_j) D_{mk}^{j*}(\alpha, \beta, \gamma). \quad (30)$$

The transformation matrix can be decomposed into three one dimensional transformations:

$$T_{\alpha_i\beta_j\gamma_k}^{jkm} = K_{\beta_j}^{jkm} L_{\alpha_i}^m M_{\gamma_k}^k, \quad (31)$$

where one dimensional transformations are defined as

$$K_{\beta_j}^{jkm} = \sqrt{\frac{2j+1}{2}} \sqrt{w_{\beta_j}} d_{mk}^j(\cos\beta_j), \quad (32)$$

$$L_{\alpha_i}^m = \frac{e^{im\alpha_i}}{\sqrt{N_\alpha}}, \quad (33)$$

$$M_{\gamma_k}^k = \frac{e^{ik\gamma_k}}{\sqrt{N_\gamma}}. \quad (34)$$

On the other hand, the transformation matrix is not a direct product of the one dimensional transformations given above, because the transformation matrix describing the transformation from the basis of $d_{mk}^j(\cos\beta)$ functions to the grid basis in $\cos\beta$ depends parametrically to the values of k and m . For this reason, the transformation from the $d_{mk}^j(\cos\beta)$ functions to the grid in $\cos\beta$ should be done first. Then, the resulting intermediate basis becomes decoupled, and the transformation from this intermediate basis to the three dimensional grid basis becomes a two dimensional Fourier transformation. This idea is suggested and used by Leforestier and co-workers in their water dimer paper [20].

TABLE VII: Transformation Properties of Euler angles under the effect of the symmetry operations of the G_{16} permutation inversion group.

E	$\alpha_1, \beta_1, \gamma_1$	$\alpha_2, \beta_2, \gamma_2$
E^*	$\pi - \alpha_1, \beta_1, -\gamma_1$	$\pi - \alpha_2, \beta_2, -\gamma_2$
(12)	$\alpha_1, \beta_1, \pi + \gamma_1$	$\alpha_2, \beta_2, \gamma_2$
(34)	$\alpha_1, \beta_1, \gamma_1$	$\alpha_2, \beta_2, \pi + \gamma_2$
$(ab)(13)(24)$	$-\alpha_2, \pi - \beta_2, \pi + \gamma_2$	$-\alpha_1, \pi - \beta_1, \pi + \gamma_1$

V. GENERATION OF BASES FOR THE SECOND MONOMER

Since the bases of the second monomer will be generated from the bases of the first monomer. The primitive functional basis of the second monomer will also be Wigner rotation functions. Thus, the primitive basis of the angular problem will be the direct product of two symmetric top bases: $|jkm\rangle \otimes |jkm\rangle$. These basis functions can be written in terms of Wigner rotation functions as

$$|j_1 k_1 m_1 j_2 k_2 m_2\rangle = \frac{\sqrt{(2j_1 + 1)(2j_2 + 1)}}{8\pi^2} D_{m_1 k_1}^{j_1*}(\alpha_1, \beta_1, \gamma_1) D_{m_2 k_2}^{j_2*}(\alpha_2, \beta_2, \gamma_2) \quad (35)$$

where $(\alpha_i, \beta_i, \gamma_i)$ are the Euler angles of the monomer i with respect to the body fixed frame of the dimer.

In order to find the effect of the symmetry operations to the basis functions, it is necessary to find the transformation properties of Euler angles under the action of symmetry operations. The effect of the symmetry operations to the Euler angles are given by Althorpe and Clary [17]. However, their definition of the body fixed axis for the monomers is different from the one used here. In their definition the water molecule is in the zy plane, while here the water molecule is in the xz plane. For that reason, the transformation properties of the Euler angles are re-derived. The difference between the transformations they have and the transformations given here is only in the effect of the E^* operation. Transformation properties of Euler angles is given in table VII. For a discussion of the derivations see appendix A.

By using the symmetry properties of the Wigner rotation functions, the effect of the symmetry operations to primitive basis functions can be found easily. The results are sum-

TABLE VIII: Effects of the symmetry operations to symmetric top basis functions.

E	$ j_1 k_1 m_1 j_2 k_2 m_2\rangle$
E^*	$(-)^{k_1+k_2} j_1 \bar{k}_1 \bar{m}_1 j_2 \bar{k}_2 \bar{m}_2\rangle$
(12)	$(-)^{k_1} j_1 k_1 m_1 j_2 k_2 m_2\rangle$
(34)	$(-)^{k_2} j_1 k_1 m_1 j_2 k_2 m_2\rangle$
$(ab)(13)(24)$	$(-)^{j_1+j_2} j_2 k_2 \bar{m}_2 j_1 k_1 \bar{m}_1\rangle$

marized in table VIII.

As discussed in the first paper, the bases of the second monomer should be generated from the bases of the first monomer by using the generator of the group that contains the permutations of the identical monomers. For water dimer the generator of the group that contains the permutations of the monomers is the operation $(ab)(13)(24)$. The effect of this operation to the Euler angles and to the primitive bases are given in tables VII and VIII, respectively.

If the i^{th} basis function belonging to the irreducible representation Γ of the group $C_{2v}(M)$ of the monomer a has the form

$$\Gamma_i^{(a)} = \sum_l C_i^l |j_l k_l m_l\rangle; \quad (36)$$

then, the corresponding basis function belonging to the representation Γ of the group $C_{2v}(M)$ of monomer b will have the form

$$\Gamma_i^{(b)} = (ab)(13)(24)\Gamma_i^{(a)} = \sum_l (-1)^{j_l} C_i^l |j_l k_l \bar{m}_l\rangle. \quad (37)$$

Although, the equations above are written for primitive basis functions, it is obvious that they apply to the symmetry adapted basis functions given in table V.

It is also necessary to generate a grid basis for the monomer b , from the grid basis of monomer a . This will be done in the same way that the spectral basis of monomer b is generated from the spectral basis of monomer a . Thus, in order to generate a grid basis for the monomer b the operation $(ab)(13)(24)$ should be applied to the grid basis functions of the monomer a .

TABLE IX: This table shows which monomer bases should be combined for obtaining bases for the water dimer calculations with the group G_{16} . In the table, labels of the irreducible representations are used to imply basis functions belonging to that symmetry. For an explanation of how to obtain mutually orthogonal basis for the doubly degenerate levels (i.e. E_x^+ , E_y^+) see reference [76].

G_{16}	Bases	G_{16}	Bases
A_1^+	$(A_1 \otimes A_1) \oplus (A_2 \times A_2)$	A_1^-	$(A_1 \otimes A_2) \oplus (A_2 \otimes A_1)$
A_2^+	$(B_1 \otimes B_1) \oplus (B_2 \otimes B_2)$	A_2^-	$(B_1 \otimes B_2) \oplus (B_2 \otimes B_1)$
B_1^+	$(A_1 \otimes A_1) \oplus (A_2 \otimes A_2)$	B_1^-	$(A_1 \otimes A_2) \oplus (A_2 \otimes A_1)$
B_2^+	$(B_1 \otimes B_1) \oplus (B_2 \otimes B_2)$	B_2^-	$(B_1 \otimes B_2) \oplus (B_2 \otimes B_1)$
E_x^+	$(A_1 \otimes B_2) \oplus (A_2 \otimes B_1)$	E_x^-	$(A_1 \otimes B_1) \oplus (A_2 \otimes B_2)$
E_y^+	$(B_2 \otimes A_1) \oplus (B_1 \otimes A_2)$	E_y^-	$(B_1 \otimes A_1) \oplus (B_2 \otimes A_2)$

If $|\alpha_i^{(a)}, \beta_j^{(a)}, \gamma_k^{(a)}\rangle$ is a grid basis function of monomer a , then the corresponding grid basis function, $|\alpha_i^{(b)}, \beta_j^{(b)}, \gamma_k^{(b)}\rangle$, of the monomer b will be

$$|\alpha_i^{(b)}, \beta_j^{(b)}, \gamma_k^{(b)}\rangle = (ab)(13)(24)|\alpha_i^{(a)}, \beta_j^{(a)}, \gamma_k^{(a)}\rangle. \quad (38)$$

The transformation properties of the Euler angles, given in table VII, says that the transformation properties of Euler angles under the operation of the permutation operation $(ab)(13)(24)$ is given by

$$(ab)(13)(24)(\alpha_1, \beta_1, \gamma_1, \alpha_2, \beta_2, \gamma_2) = (-\alpha_2, \pi - \beta_2, \pi + \gamma_2, -\alpha_1, \pi - \beta_1, \pi + \gamma_1). \quad (39)$$

Therefore, if a grid basis function of the monomer a is localized around the point $(\alpha_i, \beta_i, \gamma_i)$, then the corresponding grid basis function for the monomer b will be localized around the point $-\alpha_i, \pi - \beta_i, \pi + \gamma_i$. The effect of the permutation operation $(ab)(13)(24)$ to the Euler angles of the monomers is to relabel the angles so that they belong to monomer b , and to change the point the basis function is localized. Thus, this operation also mixes the order of the DVR functions.

VI. COMBINING MONOMER BASES

In the first paper, the way to combine monomer bases for water dimer is discussed and the bases that should be used for each symmetry are found. The results are given in table IX. Thus, after choosing the right bases for each symmetry, the basis functions can be symmetry adapted to an irreducible representation Γ of the group G_{16} which is the molecular symmetry group of the water dimer by application of the projection operator

$$P = \frac{1}{2}(E + \chi^\Gamma[(ab)(13)(24)]^*(ab)(13)(24)), \quad (40)$$

where $\chi^\Gamma[(ab)(13)(24)]$ is the character of the permutation operation $(ab)(13)(24)$ in the irreducible representation Γ . These characters can be found in the character table of the group G_{16} which is given in table X.

In order to illustrate symmetry adaptation of the basis functions, consider the irreducible representation A_1^+ . Table IX says that the bases that should be used in the calculations should be $(A_1 \otimes A_1) \oplus (A_2 \otimes A_2)$. Therefore, the basis that will be used in the calculations of the A_1^+ levels is formed by taking a direct product of the A_1 basis for monomer a and the A_1 basis for monomer b and combining this with the direct product of the A_2 basis for monomer a and the A_2 basis for monomer b . If $A_{1i}^{(a)}$ is the i^{th} basis function which has the A_1 symmetry for the monomer a , and $A_{1i}^{(b)}$, $A_{2i}^{(a)}$, $A_{2i}^{(b)}$ are defined similarly; then, the basis functions of A_1^+ calculation before the symmetry adaptation to the permutation group $G_2^{(ab)}$ will be in the form of either

$$\psi_{ij}^{(A_1^+)} = A_{1i}^{(a)} A_{1j}^{(b)}, \quad (41)$$

or

$$\psi_{ij}^{(A_1^+)} = A_{2i}^{(a)} A_{2j}^{(b)}. \quad (42)$$

After the symmetry adaptation to the permutation group $G_2^{(ab)}$, the form of the basis functions will be either

$$\Psi_{ij}^{(A_1^+)} = A_{1i}^{(a)} A_{1j}^{(b)} + A_{1j}^{(a)} A_{1i}^{(b)}, \quad (43)$$

or

$$\Psi_{ij}^{(A_1^+)} = A_{2i}^{(a)} A_{2j}^{(b)} + A_{2j}^{(a)} A_{2i}^{(b)}. \quad (44)$$

Thus, the symmetry adaptation reduces the sizes of both the $(A_1^{(a)} \otimes A_1^{(b)})$ basis and the $(A_2^{(a)} \otimes A_2^{(b)})$ basis to the half of their original size. The sign between the two terms on the

TABLE X: Character table of the G_{16} PI group. This group is isomorphic to the D_{4h} point group. In the table, $\Gamma = x \otimes y$ means that the irreducible representation Γ of the group G_{16} is the direct product of the irreducible representation x of the group G_8 , which is the pure permutation subgroup of the water dimer, and the irreducible representation y of the inversion group ε , whose character table is given in table III. This character table is taken from the reference [58]. The correlations between the irreducible representations of the group G_{16} with the irreducible representations of its subgroups G_8 and ε are added by the author.

	(12)	(ab)(13)(24)	(ab)(1324)	(12)*	(ab)(13)(24)*	(ab)(1324)*				
$G_{16} = G_8 \otimes \varepsilon$	E	(34)	(ab)(14)(23)	(ab)(1423)	(12)(34)	E^*	(34)*	(ab)(14)(23)*	(ab)(1423)*	(12)(34)*
$A_1^+ = A_1 \otimes G$	1	1	1	1	1	1	1	1	1	1
$A_2^+ = A_2 \otimes G$	1	-1	-1	1	1	1	-1	-1	1	1
$B_1^+ = B_1 \otimes G$	1	1	-1	-1	1	1	1	-1	-1	1
$B_2^+ = B_2 \otimes G$	1	-1	1	-1	1	1	-1	1	-1	1
$E^+ = E \otimes G$	2	0	0	0	-2	2	0	0	0	-2
$A_1^- = A_1 \otimes U$	1	1	1	1	1	-1	-1	-1	-1	-1
$A_2^- = A_2 \otimes U$	1	-1	-1	1	1	-1	1	1	-1	-1
$B_1^- = B_1 \otimes U$	1	1	-1	-1	1	-1	-1	1	1	-1
$B_2^- = B_2 \otimes U$	1	-1	1	-1	1	-1	1	-1	1	-1
$E^- = E \otimes U$	2	0	0	0	-2	-2	0	0	0	2

right hand side of the equation is plus because the character of the $(ab)(13)(24)$ operation in the A_1^+ representation is +1.

Equations (41) and (42) apply to the B_1^+ irreducible representation as well as it can be seen from table IX. However, symmetry adapted combinations will be different of course. Since the character of the $(ab)(13)(24)$ operation for the B_1^+ operation is -1 , symmetry adapted basis functions will be in the form of either

$$\Psi_{ij}^{(B_1^+)} = A_{1i}^{(a)} A_{1j}^{(b)} - A_{1j}^{(a)} A_{1i}^{(b)}, \quad (45)$$

or

$$\Psi_{ij}^{(B_1^+)} = A_{2i}^{(a)} A_{2j}^{(b)} - A_{2j}^{(a)} A_{2i}^{(b)}. \quad (46)$$

When the same procedure is applied to the A_2^- representation, the form of the basis functions before the symmetry adaptation becomes either

$$\psi_{ij}^{(A_2^-)} = B_{1i}^{(a)} B_{2j}^{(b)}, \quad (47)$$

or

$$\psi_{ij}^{(A_2^-)} = B_{2i}^{(a)} B_{2j}^{(b)}. \quad (48)$$

After the symmetry adaptation one gets

$$\Psi_{ij}^{(A_2^-)} = B_{1i}^{(a)} B_{2j}^{(b)} - B_{2j}^{(a)} B_{1i}^{(b)}. \quad (49)$$

Thus, in this case symmetry adaptation will mix the two different parts. So that one can take either the first product basis ($B_1^{(a)} \otimes B_2^{(b)}$) or the second product basis ($B_2^{(a)} \otimes B_1^{(a)}$) and symmetry adapt it to get the full basis. Since symmetry adaptation mixes these two different product bases with each other, only one of them is sufficient to make a symmetry adapted calculation.

Symmetry adapted bases for all of the other symmetries can be constructed similarly. It should also be noted that since the character of the operation $(ab)(13)(24)$ is 0 for the doubly degenerate levels, the projection operator given in equation (40) is nothing but the identity operation. Therefore, once the basis functions are formed, they are already symmetry adapted as they are and there is no further symmetry adaptation. In table IX, two separate bases are shown for the doubly degenerate levels which are labeled with subscripts x and y . These bases are orthogonal to each other and they do not mix with each other. In order to solve the eigenvalue problem for the doubly degenerate levels either bases can be used. They will have the same spectrum. The fact that there are two different bases for a doubly degenerate level that do not mix with each other but still give the same set of eigenvalues is the physical explanation of the double degeneracy, of course.

VII. ANGULAR CALCULATIONS

In order to solve the eigenvalue problem for five dimensional angular problem. It is necessary to evaluate the matrix elements of the angular Hamiltonian given in equation

(9). Since the contracted basis functions of the monomers are already the eigenstates of the model Hamiltonians, their evaluation is easy. The term $\Delta\hat{K}$ in that equation can be evaluated in the primitive basis of the monomers easily, and then can be transformed to the contracted bases of the monomers by using the transformation matrix which is obtained by solving the eigenstates of the model Hamiltonian's of the monomers. The term $\Delta\hat{V}$, can be evaluated easily in the grid basis which is a tensor product of the monomer grid bases, and then can be transformed to the contracted bases of monomers in two steps first by transforming from grid basis to the primitive functional basis and then transforming from the primitive functional basis to the angular basis which is the tensor product of the contracted bases of the monomers.

VIII. RADIAL CALCULATION

Once the angular problem is solved at several fixed R values, the eigenvalues for the full problem can be found by fitting the results of the angular calculations to a Morse function and solving for the eigenvalues. The Hamiltonian for this one dimensional problem becomes

$$\hat{H} = -\frac{1}{2\mu R} \frac{\partial^2}{\partial R^2} + V(R), \quad (50)$$

where $V(R)$ is the Morse function which approximates the eigenvalues of the angular calculations at the given R values. Since the Morse potential, given in the form,

$$V(r) = D(e^{-2\alpha(r-r_0)} - 2e^{-\alpha(r-r_0)}), \quad (51)$$

includes three parameters, D , α , r_0 ; it is sufficient to solve the angular problem at three different R values. If only three points are used, there exist a unique function which fits to the given data. If the calculation is done at more than three points, then the Morse function which fits to the data can be found by making a least squares fit.

When the Morse fit to the function is done, the eigenvalues of the Hamiltonian, given in equation (50), can be found easily; since for $J = 0$, the eigenvalues are analytic. According to Landau and Lifschitz, the eigenvalue of the n^{th} level is given by [77]

$$E_n = -D \left(1 - \frac{\alpha}{\sqrt{2\mu D}} \left(n + \frac{1}{2} \right) \right)^2, \quad (52)$$

where n takes integral values from zero to the greatest value for which the expression in the parentheses is positive.

IX. DETAILS OF CALCULATIONS

The calculations are done by using the SAPT-5st potential surface developed by Groenenboom *et. al.* [23, 24]. The source code of this potential surface was made available to public by Groenenboom *et. al.* [39] as an EPAPS document with the document number EPAPS:E-PRLTAO-84-060018. The source code can be obtained via ftp from the site ftp.aip.org under the directory /epaps/. The mass of H_2O is taken as 18.010560 and the moments of inertia of water monomers are taken as $A = 27.8806\text{cm}^{-1}$, $B = 14.5216\text{cm}^{-1}$ and $C = 9.2778\text{cm}^{-1}$. These values are the same with the values that are used in the original calculations of Groenenboom *et. al.*

While doing the calculations primitive functional basis of the monomers are taken as symmetric top basis with $j \leq 10$ and $m \leq 8$. Before the symmetry adaptation this corresponds to a basis size of ≈ 1650 . The number of the grid points in α and γ are set to 26 and the number of grid points in beta are set to 15 before symmetry adaptation. All of the calculations are done for $J = 0$.

In monomer calculations, the spectral basis is fully symmetry adapted and the grid basis is symmetry adapted to the permutation of the protons but not to the inversion symmetry. The matrix representing the Hamiltonian operator in the symmetry adapted symmetric top basis is stored in memory, and the diagonalization is done directly.

While doing the angular calculations, the angular basis which is obtained as a tensor product of the contracted bases of the monomers is not symmetry adapted to the full symmetry of the water dimer. Instead, the calculations are done by using the Symmetry Adapted Lanczos (SAL) algorithm [78]. The use of the SAL algorithm allows one to diagonalize more than one symmetries at once. In the case of water dimer problem being considered here, SAL method made it possible to solve for the eigenvalues of the A_1^+ and B_1^+ levels together, and also A_2^- and B_2^- levels together. This results from the fact that the angular basis of the A_1^+ and B_1^+ levels and similarly the angular basis of the A_2^- and B_2^- levels are the same before symmetry adaptation (see table IX). In the case of doubly degenerate levels calculations should be done separately for each level since the bases of double degenerate levels are unique to themselves. However, use of the SAL algorithm still makes the calculations faster since in the SAL algorithm projection operators are used to get the symmetry adapted eigenfunctions.

TABLE XI: A comparison of the results of MBR calculations with the results of Groenenboom *et. al.* The results of Groenenboom *et. al.* are taken from the table III of the reference [24]. The results in the table are in cm^{-1} . MBR results are obtained by using 100 basis functions per monomer. In the table a is the splitting due to acceptor tunneling; i_1 and i_2 are the splittings between A_1^+/B_1^+ and A_2^-/B_2^- levels due to interchange tunneling.

Symmetry	Groenenboom <i>et. al.</i>	MBR
A_1^+	-1076.8643	-1075.2116
$E+$	-1076.4312	-1074.8698
B_1^+	-1076.1419	-1074.4688
A_2^-	-1065.6333	-1063.0106
E^-	-1065.2540	-1062.6818
B_2^-	-1064.9825	-1062.3926
a	11.19	12.14
i_1	0.722	0.743
i_2	0.651	0.618

Angular calculations are done at three different fixed R values which are 5.38a.u., 5.53a.u. and 5.68a.u. The ground states eigenvalues are used to define a potential surface for the stretching motion. The potential surface of the stretching motion is found by making a nonlinear fit to the Morse function by using Newton's algorithm [79].

In order to converge the results it was necessary to use 100 basis functions per monomer for the angular calculations.

X. RESULTS AND DISCUSSIONS

A comparison of the MBR results with the original calculations of Groenenboom *et. al.* is given in table XI. In the table, i_1 is the tunneling splitting due to interchange tunneling between the A_1^+ and B_1^+ levels which is calculated as

$$i_1 = E(B_1^+) - E(A_1^+), \quad (53)$$

FIG. 4: Convergence of the results of the MBR calculations with the number of angular basis functions per monomer.

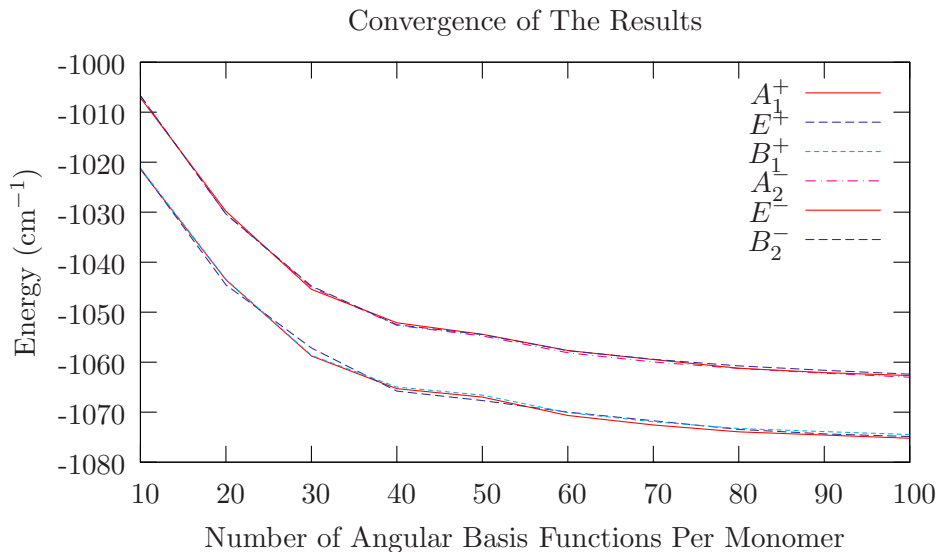
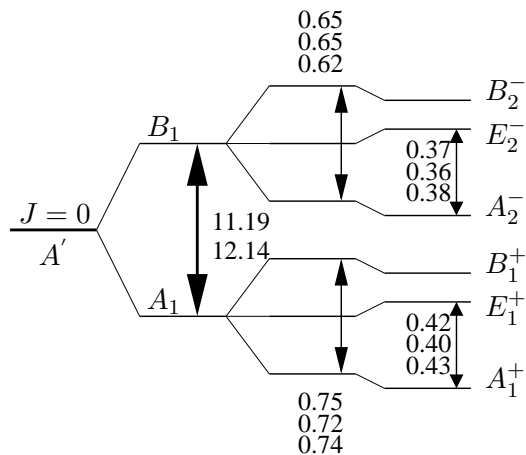


FIG. 5: A comparison of the results of MBR calculations (lower numbers) with the original calculations of Groenenboom *et. al.* (middle numbers) and the experimental data (upper numbers). Experimental data is not available for the acceptor switching.



where $E(x)$ denotes the energy of the level x ; i_2 is the interchange tunneling between the A_2^- and B_2^- levels which is calculated as

$$i_2 = E(B_2^-) - E(A_2^-); \quad (54)$$

and a is the tunneling splitting due to acceptor switching which is calculated as

$$a = \frac{E(A_1^+) + E(B_1^+)}{2} - \frac{E(A_2^-) + E(B_2^-)}{2}. \quad (55)$$

As it can be seen from the table the results are in good agreement with each other. Especially, the tunneling splittings are in very good agreement. From the table, it can be seen that the MBR calculation leads to eigenvalues which are higher than the results of Groenenboom *et. al.* This can be attributed to the fact that the stretching coordinate is treated in different ways in two calculations. In the calculations of Groenenboom *et. al.* the stretching coordinate is handled with a DVR grid with 49 equally spaced points [24]. On the other hand, in the MBR calculations stretching coordinate is separated from the angular coordinates adiabatically. Therefore, because of this difference the calculations of Groenenboom *et. al.* are less approximate than the MBR calculations. The adiabatic separation of the stretching coordinate from the angular coordinates was first done by Althorpe and Clary [17]. Their calculations are done with a different potential surface. A comparison of their results with other less approximate calculations which is done with the same potential surface is available [22]. The comparisons shows that adiabatic approximation is successful in predicting the tunneling splittings. The MBR results also shows that it is possible to get good results with adiabatic approximation.

Convergence of the results with the number of basis functions per monomer that is used in the angular calculations is shown in figure 4. The comparisons of the MBR results with the results of Groenenboom *et. al.* and the experimental data [11, 12, 15] is also shown schematically in figure 5.

From the comparison of the MBR results with the original results, it can be said that the MBR method gives good results. Since the number of the optimized basis functions that are used for each monomer (100) is much more smaller than the number of the primitive basis functions (≈ 1650), it can also be said that the method is efficient.

If the calculations were done with the same primitive bases but without generation of any optimized bases, it would be possible to decrease the size of the basis by a factor of 16 with the help of standard symmetry adaptation procedures since the molecular symmetry group of water dimer is of the order of 16. On the other hand, the use of the MBR method decreases the size of the basis of a single monomer with almost the same factor so that the size of the cluster basis becomes about 16 times smaller than what one would be able to

achieve with standard symmetry adaptation procedures.

The calculations given here can be improved in several ways. Firstly, the stretching coordinate can be treated more accurately. This can be achieved either by using more points to find the Morse potential or using more exact ways to handle it as Groenenboom *et. al.* have done or by using sequential diagonalization truncation schemes. However, this does not really seem to be necessary since the results are quite successful. Secondly, from figure 4, it can be seen that the convergence of the results is not uniform. The changes in the results when the number of angular basis functions per monomer is increased from 50 to 60 are greater than the changes in the results when the number of angular basis functions per monomer is increased from 40 to 50. This shows that simply taking the states with the lowest energies as a contracted basis is not a good idea. It might be possible to devise better strategies while forming the contracted bases in order to obtain the best possible contracted basis. Although, this does not seem to be a big problem for a six dimensional system, it might be important when one wants to study higher dimensional systems.

XI. CONCLUSIONS

Application of the MBR method has been illustrated by calculating the VRT spectra of water dimer by using the SAPT-5st potential surface of Groenenboom *et. al.* [24]. The calculations are done by using Wigner rotation functions as primitive bases. The use of the MBR method made it possible to decrease size of monomer bases by a factor of ≈ 16 . The results of the calculations are in good agreement with both the original calculations of Groenenboom *et. al.* and also with the experimental results. A detailed discussion of the results can be found in section X.

Because of its efficiency, the MBR method can be used for studies of clusters bigger than dimers. Thus, it can be used for studying the many-body terms and for deriving accurate potential surfaces. The results of calculations in this paper are especially encouraging for a study of water trimer with a pairwise potential surface. For example: consider the nine dimensional Hamiltonian derived by van der Avoird *et. al.* [48]. In that model, all of the monomers are allowed to rotate around their center of masses but the center of masses of monomers are fixed in space. If the trimer calculation would require about the same number of contracted basis functions for a monomer, then a study of the nine dimensional angular

problem of water trimer would require 10^6 basis functions. Although, a problem of that size can be handled with iterative methods, it is still quite big. Nevertheless, it is reasonable to expect that the trimer problem can be solved with less number of optimized basis functions per monomer. Firstly, water trimer is much more symmetric than water dimer. Secondly, a study of water trimer with a pairwise potential surface will have much deeper potential wells. Because of the importance of the three-body terms in the potential surface of water trimer, a calculation with a pairwise potential surface cannot give an accurate estimation of the experimental data. Nevertheless, this should be a big step towards the derivation of three-body terms in the potential surface of bulk liquid and solid water. A qualitative model for a possible application of the MBR method to water trimer is already given in the first paper. Its implementation remains as a future work.

Appendix A: A Simple Way to Find The Transformation Properties of Euler Angles

The transformation properties of the Euler angles of a body fixed frame under rotations is well known if the Euler angles are defined with respect to a space fixed frame, which does not move under the effect of any symmetry operation. These transformations are given in the book *Molecular Symmetry and Spectroscopy*, written by Bunker and Jensen [59]. For convenience of the reader, they are given in table XII. However, the case of the small clusters is different, because the Euler angles of the body fixed frames of the monomers are defined with respect to the body fixed frame of the cluster, and not with respect to a space fixed frame. Since the body fixed frame of the cluster is not fixed in space, it also rotates with the effects of permutation inversion operations. Therefore, the application of the transformations given in table XII is sufficient only if the body fixed frame of the cluster does not move. However, they will give wrong answers if the body fixed frame of the cluster moves, too. For example, in the case of water dimer, transformations given in table XII will give the right answer for the operation of (12). However, they will not work for the operations E^* and $(ab)(13)(24)$, because these operations rotate the body fixed frame of the dimer around its x axis by π radians.

To the best of author's knowledge there is not any easy way of finding the transformations in these cases available in the literature. In the following lines, an easy way of finding these transformations will be discussed.

TABLE XII: Transformation properties of Euler Angles. This table is taken from page 266 of the book *Molecular Symmetry and Spectroscopy* written by Bunker and Jensen [59]. Coordinates are relabeled to make it consistent with notation used here. In the table, R_ϕ^π is a rotation of the molecule fixed (x, y, z) axes through π radians about an axis in the xy plane making an angle ϕ with the x axis (ϕ is measured in the right hand sense about the x axis), and R_z^θ is a rotation of molecule fixed (x, y, z) axes through θ radians about z axis (θ is measured in the right hand sense about the z axis).

	R_ϕ^π	R_z^θ
β	$\pi - \beta$	β
α	$\alpha + \pi$	α
γ	$2\pi - 2\phi - \gamma$	$\gamma + \theta$

In order to find the changes in the Euler angles, the process will be divided into two steps. In the first step the orientation of the body fixed frame of the monomers will be kept fixed with respect to a space fixed frame. However, the body fixed frame of the cluster will be rotated together with the body, of course. In the second step, the rotation of the monomer frames will be done.

The transformations in the second step will be the same with the ones given in table XII, because the cluster frame does not move in the second step. Therefore, if one finds the transformations for the first step, then the overall transformation can be found by applying two transformations sequentially.

The transformation properties of the first step can be found easily by realizing that the only difference in the first step is that the roles of the two frames are interchanged. This time, it is the monomer frame which acts like the space fixed frame since it doesn't move; and it is the cluster frame that rotates. If (α, β, γ) are the Euler angles of the monomer frame defined with respect to the cluster frame, one can equally say that $(-\gamma, -\beta, -\alpha)$ are the Euler angles of the cluster frame defined with respect to the monomer frame. Thus, the Euler angles of the cluster frame with respect to the monomer frame after the rotation can be found by applying the transformations in table XII. Then, the Euler angles of the monomer frame with respect to the cluster frame can be found by using the same trick

TABLE XIII: Transformation properties of Euler Angles. Definitions of the rotation operations are the same with table XII. However, this time it is the cluster frame rotating, not the monomer frame.

	R_ϕ^π	R_z^θ
β	$\pi - \beta$	β
α	$2\phi - \alpha$	$\alpha - \theta$
γ	$\pi + \gamma$	γ

again. If $(\alpha', \beta', \gamma')$ are the Euler angles of the cluster frame obtained by applying the transformations in table XII to the Euler angles $(-\gamma, -\beta, -\alpha)$, then the Euler angles of the monomer frame will be $(-\gamma', -\beta', -\alpha')$.

Thus, by using the transformation rules given in table XII, one can find the transformation properties of Euler angles of the monomer when it is only the frame of the cluster that rotates. The general formulas for such transformations are derived and the results are summarized in table XIII.

Since the order of the two successive operations that are used to find the transformation properties of the Euler angles of the monomer is not important for the final orientation of the frames, the order in which one uses the transformations is not important.

To illustrate the applications of the transformations given in tables XII, and XIII, to molecular clusters, consider water dimer. Body fixed frames of the dimer and the monomers are given in figures 2 and 3, respectively. Firstly, consider the effect of E^* operation to water dimer. This operation rotates the body fixed frame of the monomer around its y axis by π radians (see figure 3) and it also rotates the body fixed frame of the dimer around its x axis by π radians (see figure 2). By using the transformations in table XII (with $\phi = \pi/2$), the effect of the monomer rotation to the Euler angles is found to be

$$(\alpha, \beta, \gamma) \rightarrow (\pi + \alpha, \pi - \beta, \pi - \gamma). \quad (\text{A1})$$

Then, by using the transformations in table XIII (with $\phi = 0$) the effect of rotation of the dimer frame to the Euler angles of the monomer frame is found to be

$$(\pi + \alpha, \pi - \beta, \pi - \gamma) \rightarrow (\pi - \alpha, \beta, -\gamma,) \quad (\text{A2})$$

where $-\alpha - \pi$ is replaced with $\pi - \alpha$. This is possible because adding 2π to the angles α and γ doesn't change anything since they have a period of 2π . Therefore, the overall transformation becomes,

$$(\alpha, \beta, \gamma) \rightarrow (\pi - \alpha, \beta, -\gamma). \quad (\text{A3})$$

This is what is reported in table VII. The same transformation applies to both of the monomers.

In the case of the operation $(ab)(13)(24)$, the effect of the operation to the monomer frames is just to relabel them, so the first transformation becomes

$$(\alpha_1, \beta_1, \gamma_1, \alpha_2, \beta_2, \gamma_2) \rightarrow (\alpha_2, \beta_2, \gamma_2, \alpha_1, \beta_1, \gamma_1). \quad (\text{A4})$$

This operation also rotates the dimer frame around its x axis by π radians, so with the transformations given in table XIII, one gets

$$(\alpha_2, \beta_2, \gamma_2, \alpha_1, \beta_1, \gamma_1) \rightarrow (-\alpha_2, \pi - \beta_2, \pi + \gamma_2, -\alpha_1, \pi - \beta_1, \pi + \gamma_1). \quad (\text{A5})$$

Therefore, the overall effect of the $(ab)(13)(24)$ operation to the Euler angles of the monomers become

$$(\alpha_1, \beta_1, \gamma_1, \alpha_2, \beta_2, \gamma_2) \rightarrow (-\alpha_2, \pi - \beta_2, \pi + \gamma_2, -\alpha_1, \pi - \beta_1, \pi + \gamma_1). \quad (\text{A6})$$

The symmetry operations (12) and (34) do not have any effect on the body fixed frame of the dimer. Therefore, their effect to the Euler angles of the monomers can be found by using the transformations given in table XII. The results will be the ones that are reported in table VII.

Appendix B: Real Symmetric Top Basis

The fact that the symmetric top basis is complex, makes the calculations more demanding, since complex numbers occupies twice the memory real numbers occupies. For this reason, it is advantageous to transform the symmetric top basis to a real basis that we will be called real symmetric top basis. The way to generate a real basis from a complex basis is obvious: sum and differentiate with its complex conjugate. By using the symmetry properties of the Wigner rotation functions [65], it can be shown easily that

$$D_{mk}^{j*}(\alpha, \beta, \gamma) = (-1)^{m-k} D_{-m-k}^j(\alpha, \beta, \gamma). \quad (\text{B1})$$

From the equation above, it follows that $|jkm\rangle^* = (-1)^{m-k}|j\bar{k}\bar{m}\rangle$. This leads to the result that the linear combinations $|jkm\rangle \pm |j\bar{k}\bar{m}\rangle$ are either pure real or pure imaginary. In the case of pure imaginary functions, the imaginary number i can be omitted since it is just a phase factor. After doing some algebra, following functions are obtained as the real symmetric top basis.

For $m - k$ is odd:

$$\frac{|jkm\rangle + |j\bar{k}\bar{m}\rangle}{i\sqrt{2 + 2\delta_{k0}\delta_{m0}}} = \frac{\sqrt{2j+1}}{2\sqrt{1 + \delta_{k0}\delta_{m0}}} \sin(m\alpha + k\gamma) d_{mk}^j(\cos\beta), \quad (\text{B2})$$

$$\frac{|jkm\rangle - |j\bar{k}\bar{m}\rangle}{\sqrt{2}} = \frac{\sqrt{2j+1}}{2\sqrt{1 + \delta_{k0}\delta_{m0}}} \cos(m\alpha + k\gamma) d_{mk}^j(\cos\beta). \quad (\text{B3})$$

For $m - k$ is even:

$$\frac{|jkm\rangle - |j\bar{k}\bar{m}\rangle}{i\sqrt{2}} = \frac{\sqrt{2j+1}}{2\sqrt{1 + \delta_{k0}\delta_{m0}}} \sin(m\alpha + k\gamma) d_{mk}^j(\cos\beta), \quad (\text{B4})$$

$$\frac{|jkm\rangle + |j\bar{k}\bar{m}\rangle}{\sqrt{2 + 2\delta_{k0}\delta_{m0}}} = \frac{\sqrt{2j+1}}{2\sqrt{1 + \delta_{k0}\delta_{m0}}} \cos(m\alpha + k\gamma) d_{mk}^j(\cos\beta). \quad (\text{B5})$$

When the real symmetric top basis functions are used as a basis, the transformation matrix elements from this basis to the grid basis also becomes real. Thus, by using equation (27), transformation matrix elements for the basis functions given by equations (B2) and (B4) becomes

$$T_{\alpha_i\beta_j\gamma_k}^{jkm} = \frac{\sqrt{2j+1}}{2\sqrt{1 + \delta_{k0}\delta_{m0}}} \frac{\sin(m\alpha_i + k\gamma_k)}{\sqrt{N_\alpha N_\gamma}} \sqrt{w_{\beta_j}} d_{mk}^j(\cos\beta_j), \quad (\text{B6})$$

and the transformation matrix elements for the basis functions given in equations (B3) and (B5) becomes

$$T_{\alpha_i\beta_j\gamma_k}^{jkm} = \frac{\sqrt{2j+1}}{2\sqrt{1 + \delta_{k0}\delta_{m0}}} \frac{\cos(m\alpha_i + k\gamma_k)}{\sqrt{N_\alpha N_\gamma}} \sqrt{w_{\beta_j}} d_{mk}^j(\cos\beta_j). \quad (\text{B7})$$

Appendix C: Kinetic Energy Matrix Elements in Water Dimer Calculations

In this appendix, the matrix elements are given for the complex symmetric top basis functions. Application of the formulas given here to the real symmetric top basis functions is straightforward.

If $|j_1k_1m_1j_2k_2m_2\rangle = |j_1k_1m_1\rangle|j_2k_2m_2\rangle$; then, the nonzero matrix elements of \hat{K}_1 is given by

$$\langle j_1k_1m_1j_2k_2m_2|\hat{K}_1|j_1k_1m_1j_2k_2m_2\rangle = \left(\frac{A+B}{2}\right) j_1(j_1+1) + \left(C - \frac{A+B}{2}\right) k_1^2, \quad (\text{C1})$$

and

$$\begin{aligned}
\langle j_1 k_1 m_1 j_2 k_2 m_2 | \hat{K}_1 | j_1 k_1 \pm 2 m_1 j_2 k_2 m_2 \rangle &= \left(\frac{B - C}{4} \right) \\
&\times \sqrt{j_1(j_1 + 1) - (k_1 \pm 2)(k_1 \pm 1)} \\
&\times \sqrt{j_1(j_1 + 1) - (k_1 \pm 1)k_1}. \quad (C2)
\end{aligned}$$

Similar expressions can be derived for \hat{K}_2 . For $J = 0$, nonzero matrix elements of \hat{K}_{12} are given by

$$\langle j_1 k_1 m_1 j_2 k_2 m_2 | \hat{K}_{12} | j_1 k_1 m_1 j_2 k_2 m_2 \rangle = \frac{1}{2\mu R^2} [j_1(j_1 + 1) + j_2(j_2 + 1) + 2m_1 m_2] \delta_{m_1, -m_2}, \quad (C3)$$

and

$$\begin{aligned}
\langle j_1 k_1 m_1 \mp 1 j_2 k_2 m_2 \pm 1 | \hat{K}_{12} | j_1 k_1 m_1 j_2 k_2 m_2 \rangle &= \frac{1}{2\mu R^2} C_{j_1, m_1}^\mp \\
&\times C_{j_2, m_2}^\pm \delta_{m_1, -m_2}, \quad (C4)
\end{aligned}$$

where

$$C_{jm}^\pm = \sqrt{j(j + 1) \pm m(m + 1)}. \quad (C5)$$

-
- [1] L. Ojamäe and K. Hermansson, *J. Phys. Chem.* **98**, 4271 (1994).
- [2] A. Millet, R. Moszynski, P. E. S. Wormer, and A. van der Avoird, *J. Phys. Chem. A* **103**, 6811 (1999).
- [3] T. R. Dyke, K. M. Mack, and J. S. Muentner, *J. Chem. Phys.* **66**, 498 (1977).
- [4] J. A. Odutola and T. R. Dyke, *J. Chem. Phys.* **72**, 5062 (1980).
- [5] L. H. Coudert, F. J. Lovas, R. D. Suenram, and J. T. Hougen, *J. Chem. Phys.* **87**, 6290 (1987).
- [6] Z. S. Huang and R. E. Miller, *J. Chem. Phys.* **91**, 6613 (1989).
- [7] Z. S. Huang and R. E. Miller, *J. Chem. Phys.* **88**, 8008 (1988).
- [8] K. L. Busarow, R. C. Cohen, G. A. Blake, K. B. Laughin, Y. T. Lee, and R. J. Saykally, *J. Chem. Phys.* **90**, 3937 (1989).
- [9] T. A. Hu and T. R. Dyke, *J. Chem. Phys.* **91**, 7348 (1989).
- [10] G. T. Fraser, R. D. Suenram, and L. H. Coudert, *J. Chem. Phys.* **90**, 6077 (1989).
- [11] G. T. Fraser, *Int. Rev. Phys. Chem.* **10**, 189 (1991).
- [12] E. Zwart, J. J. ter Meulen, W. L. Meerts, and L. H. Coudert, *J. Mol. Spec.* **147**, 27 (1991).
- [13] F. N. Keutsch, L. B. Braly, M. G. Brown, H. A. Harker, P. B. Petersen, C. Leforestier, and R. J. Saykally, *J. Chem. Phys.* **119**, 8927 (2003).
- [14] L. B. Braly, J. D. Cruzan, K. Liu, R. S. Fellers, and R. J. Saykally, *J. Chem. Phys.* **112**, 10293 (2000).
- [15] L. B. Braly, K. Liu, M. G. Brown, F. N. Keutsch, R. S. Fellers, and R. J. Saykally, *J. Chem. Phys.* **112**, 10314 (2000).
- [16] J. G. Loeser, N. Pugliano, J. D. Cruzan, and R. J. Saykally, *J. Chem. Phys.* **98**, 6600 (1993).
- [17] S. Althorpe and D. C. Clary, *J. Chem. Phys.* **101**, 3603 (1994).
- [18] S. C. Althorpe and D. C. Clary, *J. Chem. Phys.* **102**, 4390 (1995).
- [19] J. K. Gregory and D. C. Clary, *J. Chem. Phys.* **102**, 7817 (1995).
- [20] C. Leforestier, L. B. Braly, K. Liu, M. J. Elrod, and R. J. Saykally, *J. Chem. Phys.* **106**, 8527 (1997).
- [21] R. S. Fellers, L. B. Braly, R. J. Saykally, and C. Leforestier, *J. Chem. Phys.* **110**, 6306 (1999).
- [22] H. Chen, S. Liu, and J. C. Light, *J. Chem. Phys.* **110**, 168 (1999).
- [23] E. M. Mas, R. Bukowski, K. Szalewicz, G. C. Groenenboom, P. E. S. Wormer, and A. van der

- Avoird, J. Chem. Phys. **113**, 6687 (2000).
- [24] G. C. Groenenboom, P. E. S. Wormer, A. van der Avoird, E. M. Mas, R. Bukowski, and K. Szalewicz, J. Chem. Phys. **113**, 6702 (2000).
- [25] O. Matsuoka, E. Clementi, and M. Yosmine, J. Chem. Phys. **64**, 1351 (1976).
- [26] R. O. Watts, J. R. Reimers, and M. L. Klein, Chem. Phys. **64**, 95 (1982).
- [27] W. L. Jorgensen, J. Am. Chem. Soc. **103**, 335 (1981).
- [28] W. L. Jorgensen, J. Chem. Phys. **77**, 4156 (1982).
- [29] W. L. Jorgensen, J. Chandrasekhar, and J. D. Madura, J. Chem. Phys. **79**, 926 (1983).
- [30] H. J. C. Berendsen, J. R. Grigera, and T. P. Straatasma, J. Phys. Chem. **91**, 6269 (1987).
- [31] P. Cieplak, P. Kolman, and T. Lybrand, J. Chem. Phys. **92**, 6755 (1990).
- [32] C. D. Berweger, W. F. van Gunsteren, and F. Müller-Plathe, Chem. Phys. Lett. **232**, 429 (1995).
- [33] C. Millot, J. C. Soetens, M. T. C. M. Costa, M. P. Hodges, and A. J. Stone, J. Phys. Chem. A **102**, 102 (754).
- [34] T. Slee and R. J. L. Roy, J. Chem. Phys. **99**, 360 (1993).
- [35] H. Sun and R. O. Watts, J. Chem. Phys. **92**, 603 (1990).
- [36] M. Quack and M. A. Shum, J. Chem. Phys. **95**, 28 (1991).
- [37] R. Moszyniski, P. E. S. Wormer, and A. v. B. jezioriski, J. Chem. Phys. **103**, 8058 (1995).
- [38] R. Moszyniski, P. E. S. Wormer, B. Jezioriski, and A. van der Avoird, J. Chem. Phys. **107**, 672 (1997).
- [39] G. C. Groenenboom, E. M. Mas, R. Bukowski, P. E. S. W. K. Szalewicz, and A. van der Avoird, Phys. Rev. Lett. **84**, 4072 (2000).
- [40] J. Echave and D. C. Clary, Chem. Phys. Lett. **190**, 225 (1992).
- [41] F. N. Keutsch, J. D. Cruzan, and R. J. Saykally, Chem. Rev. **103**, 2533 (2003).
- [42] N. Pugliano and R. J. Saykally, Science **257**, 1937 (1992).
- [43] F. N. Keutsch and R. J. Saykally, Proc. Nat. Acad. Sci. (USA) **98**, 10533 (2001).
- [44] K. Liu, J. G. Loeser, M. J. Elrod, B. C. Host, B. C. Rzepcila, J. A. Pugliano, and R. J. Saykally, J. Am. Chem. Soc. **116**, 3507 (1994).
- [45] M. R. Viant, J. D. Cruzan, D. D. Lucas, M. G. Brown, K. Liu, and R. J. Saykally, J. Phys. Chem. A **101**, 9032 (1997).
- [46] F. N. Keutsch, R. J. Saykally, and D. J. Wales, J. Chem. Phys. **117**, 8823 (2002).

- [47] M. R. Viant, M. G. Brown, J. D. Cruzan, R. J. Saykally, M. Geleijns, and A. van der Avoird, *J. Chem. Phys.* **110**, 4369 (1999).
- [48] A. van der Avoird, E. H. T. Olthof, and P. E. S. Wormer, *J. Chem. Phys.* **105**, 8034 (1996).
- [49] E. H. T. Olthof, A. van der Avoird, P. E. S. Wormer, K. Liu, and R. J. Saykally, *J. Chem. Phys.* **105**, 8051 (1996).
- [50] M. Schütz, T. Bürgi, S. Leutwyler, and H. B. Bürgi, *J. Chem. Phys.* **99**, 5228 (1993).
- [51] C. S. Guiang and R. E. Wyatt, *Int. J. Qua. Chem.* **68**, 233 (1998).
- [52] I. M. B. Nielsen, E. T. Seidl, and C. L. Janssen, *J. Chem. Phys.* **110**, 9435 (1999).
- [53] E. M. Mas, R. Bukowski, and K. Szalewicz, *J. Chem. Phys.* **118**, 4386 (2003).
- [54] Z. Bačić, *Comp. Phys. Com.* **145**, 184 (2002).
- [55] S. S. Xantheas and T. H. D. Jr., *J. Chem. Phys.* **98**, 8037 (1993).
- [56] W. Klopper and M. Schütz, *Chem. Phys. Lett.* **237**, 536 (1995).
- [57] M. G. Brown, M. R. Viant, R. P. McLaughkin, C. J. Keoshian, E. Michael, J. D. Cruzan, R. J. Saykally, and A. van der Avoird, *J. Chem. Phys.* **111**, 7789 (1999).
- [58] T. R. Dyke, *J. Chem. Phys.* **66**, 492 (1977).
- [59] P. R. Bunker and P. Jensen, *Molecular Symmetry and Spectroscopy* (National Research Council Canada Research Press, Ottawa, 1998), 2nd ed.
- [60] P. R. Bunker and P. Jensen, *Fundamentals of Molecular Symmetry* (Institute of Physics Publishing, Bristol, 2005), 1st ed.
- [61] R. S. Fellers, C. Leforstier, L. B. Braly, M. G. Brown, and R. Saykally, *Science* **284**, 945 (1999).
- [62] G. Brocks, A. van der Avoird, B. T. Sutcliffe, and J. Tennyson, *Mol. Phys.* **50**, 1025 (1983).
- [63] H. Lee and J. C. Light, *J. Chem. Phys.* **118**, 3458 (2003).
- [64] H. Lee and J. C. Light, *J. Chem. Phys.* **120**, 4626 (2004).
- [65] M. E. Rose, *Elementary Theory of Angular Momentum* (Dover Publications Inc., New York, 1957), 1st ed.
- [66] J. C. Light, I. P. Hamilton, and J. V. Lill, *J. Chem. Phys.* **82**, 1400 (1985).
- [67] Z. Bačić and J. C. Light, *Ann. Rev. Phys. Chem.* **40**, 469 (1989).
- [68] J. C. Light and T. Carrington, Jr., *Adv. Chem. Phys.* **114**, 263 (2000).
- [69] G. C. Corey and D. Lemoine, *J. Chem. Phys.* **97**, 4115 (1997).
- [70] G. C. Corey, J. W. Tromp, and D. Lemoine (NATO ASI Series C, Dordrecht, 1993), vol. 412,

pp. 1–23.

- [71] C. Leforestier, *J. Chem. Phys.* **101**, 7357 (1994).
- [72] R. M. Whitnell and J. C. Light, *J. Chem. Phys.* **89**, 3674 (1988).
- [73] H. Wei and T. Carrington, Jr., *J. Chem. Phys.* **101**, 1343 (1994).
- [74] A. McNichols and T. Carrington, Jr., *Chem. Phys. Lett.* **202**, 464 (1993).
- [75] J. V. Lill, G. A. Parker, and J. C. Light, *Chem. Phys. Lett.* **89**, 483 (1982).
- [76] M. E. Ocak, Ph.D. thesis, The University of Chicago (2008).
- [77] L. D. Landau and E. M. Lifschitz, *Quantum Mechanics (Non-relativistic Theory)* (Butterworth-Heinemann, Oxford, 1977), 3rd ed.
- [78] X.-G. Wang and T. Carrington, Jr., *J. Chem. Phys.* **114**, 1473 (2001).
- [79] E. Isaacson and H. B. Keller, *Analysis of Numerical Methods* (Dover Publications Inc., New York, 1994), 1st ed.